Tartakoff, A., & Vassalli, P. (1978) *J. Cell Biol. 79*, 694–707.
Tartakoff, A., Vassali, P., & Detraz, M. (1979) *J. Cell Biol. 83*, 284–299.
Tartakoff, A. M., Hoessli, D., & Vassalli, P. (1981) *J. Mol. Biol. 150*, 525–535.
Uchida, N., Smilowitz, H., & Tanzer, M. L. (1979) *Proc. Natl. Acad. Sci. U.S.A. 76*, 1868–1872.
Van Obberghen, E., Kasuga, M., LeCam, A., Hedo, J. A., Itin, A., & Harrison, L. C. (1981) *Proc. Natl. Acad. Sci. U.S.A. 78*, 1052–1056.
Van Obberghen, E., Rossi, B., Kowalski, A., Gazzano, H., & Ponzio, G. (1983) *Proc. Natl. Acad. Sci. U.S.A. 80*, 945–949.
Wisher, M. H., Baron, M. D., Jones, R. H., Sonksen, P. H., Saunders, D. J., Thamm, P., & Brandenburg, D. (1980) *Biochem. Biophys. Res. Commun. 92*, 492–498.
Yeung, C. W. T., Moule, M. L., & Yip, C. C. (1980) *Biochemistry 19*, 2196–2203.

Structure of the Capsid of Kilham Rat Virus from Small-Angle Neutron Scattering†

C. R. Wobbe,‡ S. Mitra, and V. Ramakrishnan*

ABSTRACT: The structure of empty capsids of Kilham rat virus, an autonomous parvovirus with icosahedral symmetry, was investigated by small-angle neutron scattering. From the forward scatter, the molecular weight was determined to be 4.0×10^6, and from the Guinier region, the radius of gyration was found to be 105 Å in D_2O and 104 Å in H_2O. On the basis of the capsid molecular weight and the molecular weights and relative abundances of the capsid proteins, we propose that the capsid has a triangulation number of 1. Extended scattering curves and mathematical modeling revealed that the capsid consists of two shells of protein, the inner shell extending from 58 to 91 Å in D_2O and from 50 to 91 Å in H_2O and containing 11% of the capsid scattering mass, and the outer shell extending to 121 Å in H_2O and D_2O. The inner shell appears to have a higher content of basic amino acids than the outer shell, based on its lower scattering density in D_2O than in H_2O. We propose that all three capsid proteins contribute to the inner shell and that this basic region serves DNA binding and partial charge neutralization functions.

The mammalian parvoviruses are among the smallest animal viruses known with a linear single-stranded (ss)[1] DNA genome of approximately 5000 bases and an icosahedral capsid of 22-nm diameter. They are classified in two subgroups, the defective parvoviruses (including adeno-associated virus), which require coinfection by helper virus for replication, and the nondefective or autonomous parvoviruses (including KRV, H-1, and MVM), which have no helper requirement. In general, the autonomous parvoviruses mentioned share very similar properties in terms of capsid structure and composition (Peterson et al., 1978; Tattersall & Ward, 1978).

The capsid of KRV consists of three proteins—A, B, and C—with apparent masses of 80, 64, and 59 kilodaltons, respectively (Mitra et al., 1982). In MVM, these three proteins appear to share extensive sequence homology on the basis of two-dimensional peptide mapping (Tattersall et al., 1977). This is consistent with other experimental evidence indicating that (i) messages for polypeptides A and B are transcribed from overlapping regions of the viral genome in H-1 (Rhode & Paradiso, 1983) and (ii) protein C is generated by proteolytic cleavage of protein B during the maturation of DNA-containing, full virions (Clinton & Hayashi, 1975, 1976). The cleavage of protein B is accompanied by a decrease in the virion's buoyant density in CsCl and an increase in infectivity.

The A protein is particularly interesting for two reasons. First, it is present in both empty and full capsids in roughly a constant proportion relative to protein B and C (see below) (Tattersall et al., 1976). Moreover, A does not undergo proteolytic cleavage, unlike B, despite the fact that the B sequence is contained within A (Tattersall et al., 1977). Second, the region of the A protein that does not overlap with B or C is known to contain highly basic peptides that give A a much more basic p*I* than B or C (Mitra et al., 1982; Tattersall et al., 1976). Together, these observations suggest a conformation-specific functional role for protein A in the virus capsid, possibly in DNA binding and partial charge neutralization.

To date, little work has been done on the three-dimensional structure of parvoviruses. Early electron microscope observations of KRV and H-1 (Vasquez & Brailousky, 1965; Karasaki, 1966) indicated that the capsid is an icosahedron with 32 capsomers, and therefore had a triangulation number of 3. Later investigations (Tattersall et al., 1976) concluded that there are about 64 protein molecules per capsid, and hence the capsomeres are dimeric. On the basis of the apparent molar ratios of the proteins, it was proposed that empty capsids contain 8 or 9 molecules of A and 53–57 molecules of B. Full particles were found to contain 8–9 molecules of protein A and total of 53–57 molecules of B plus C proteins combined (Tattersall et al., 1976).

† From the University of Tennessee—Oak Ridge Graduate School of Biomedical Sciences and Biology Division, and the National Center for Small Angle Scattering Research, Oak Ridge National Laboratory, Oak Ridge, Tennessee 37831. *Received March 6, 1984.* Research sponsored by the Office of Health and Environmental Research, U.S. Department of Energy, under Contract DE-AC05-84OR21400 with the Martin Marietta Energy Systems, Inc.

* Address correspondence to this author at the Biology Department, Brookhaven National Laboratory, Upton, Long Island, NY 11973.

‡ Supported by NIH Training Grant 7438.

[1] Abbreviations: ss, single stranded; AAV, adeno-associated virus; MVM, minute virus of mice; KRV, Kilham rat virus; kDa, kilodalton(s); Tris-HCl, tris(hydroxymethyl)aminomethane hydrochloride; EDTA, ethylenediaminetetraacetic acid.

0006-2960/84/0423-6565$01.50/0

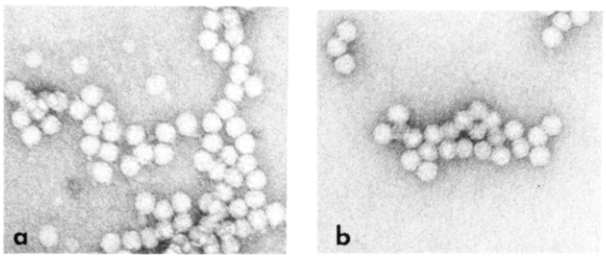

FIGURE 1: Electron micrographs of full virions (a) and empty capsids (b) of KRV. Capsids were stained with 2% uranyl acetate in 0.1 M Na/glycine buffer (pH 8.0) prior to spreading. Magnification, 100000×.

Small-angle neutron scattering has proven to be a useful tool for the study of a number of icosahedral viruses in solution (Jacrot, 1981). We have examined the structure of empty capsids of KRV using this technique and propose a model for the radial distribution of protein in empty capsids at 40-Å resolution. We also suggest a revised triangulation number and possible roles for the capsid proteins based on this model.

Materials and Methods

Cells and Virus. Normal rat kidney (NRK) cells (Doc-Nguyen et al., 1966), strain N153, kindly provided by W. K. Yang of this division, were maintained in Eagle's minimum essential medium plus 10% fetal calf serum (GIBCO). KRV strain 171 has been described previously (Mitra et al., 1982).

Virus Infection and Purification of Empty Capsids. Cultures of NRK cells in roller bottles were infected at about 20% confluence in serum-free medium, and 1 h later the medium was adjusted to 10% fetal calf serum. After 96 h growth at 37 °C, the cells were scraped, pelleted, and resuspended in 20 mM Tris-HCl, pH 8.0. The cells were then lysed, and virus was obtained as previously described (Mitra et al., 1982), except that protease treatment was omitted and the extract was made to 0.5% Sarkosyl (CIBA-Geigy) and 10 mM EDTA after nuclease treatment.

Empty capsids recovered from the first round of equilibrium sedimentation in CsCl ($\rho \simeq 1.32$) were layered on a step gradient of 30% and 35% CsCl (w/w) and rebanded at 33000 rpm for 18 h at 15 °C in the SW 41 rotor (Beckman). Complete empty capsids were separated from partially assembled capsids and adventitiously associated proteins by chromatography on Bio-Gel A-5m (Bio-Rad). The capsids were concentrated by pelleting at 400000*g* for 2 h and resuspended at the appropriate concentrations in the buffers indicated. This procedure gave homogeneous preparations of empty capsids as shown by electron microscopy (Figure 1), the ultraviolet spectrum, and the lack of [^{3}H]thymidine labeling (data not shown).

Amino Acid Analysis. For amino acid analysis, a suspension of empty capsids of known A_{280} was hydrolyzed in evacuated (<50 μmHg) sealed tubes with 6 N HCl/10 mM 2-mercaptoethanol at 110 °C for 21 h. After being dried in vacuo, hydrolysates were subjected to chromatography on a Beckman 121 M amino acid analyzer using Beckman's "3-hour-single-column system". The results are the average of duplicate analyses. Norleucine was used as an internal standard.

Neutron Scattering. Prior to scattering measurements, samples of the viral capsids were dialyzed against scattering buffer made up in H_2O or D_2O (10 mM Tris-HCl, pH 8.0, and 1 mM EDTA). The samples were then placed in cylindrical quartz cells of 1-mm thickness and 2-cm diameter obtained from Precision Cells. Scattering measurements were done on the 30-m small-angle neutron scattering instrument of the National Center for Small Angle Scattering Research at Oak Ridge National Laboratory (Koehler et al., 1981). Data were collected by a two-dimensional position-sensitive ^{3}He detector with 64 × 64 1-cm^2 channels. A collimation of 7.5 m with a source slit of 3.5 cm and a sample slit of 1.74 cm was used. The sample–detector distance was varied from about 9.0 m for the radius of gyration measurements to 3.0 m for measurements of the extended scattering curves. The flux incident on the sample was 3.5×10^4 N cm^{-2} s^{-1} with a wavelength of 4.75 Å and a wavelength spread, $\Delta\lambda/\lambda$, of 6% (full width at half-maximum). Measurements lasted between 5 and 15 h. Sample transmissions were used to determine D_2O content. In each case, the transmissions of the sample and buffer were virtually identical, thus eliminating a possible source of systematic errors.

The raw data were normalized to 1000 monitor counts, corrected for background and sensitivity, and radially averaged to give the measured intensity, $I(k)$, as a function of $k = (4\pi/\lambda) \sin 2\theta$ where 2θ is the scattering angle and λ is the wavelength. Statistical errors from counting were propagated throughout the data reduction procedure.

Data Analysis

Radius of Gyration and Forward Scatter. At low angles, Guinier's law holds (Jacrot, 1976). Guinier plots (ln I vs. k)

$$I(k) = I(0)e^{-k^2\frac{R_g^2}{3}} \quad (1)$$

of the data were used to determine the forward scatter, $I(0)$, and the radius of gyration, R_g. The plots were linear in the Guinier region and yielded the same R_g for concentrations of 3 and 20 mg/mL, showing the absence of any concentration effects in the range studied.

Because of the geometry, which was chosen to optimize flux, a certain amount of instrumental smearing is present in the data, which tends to reduce $I(0)$ and R_g. The effect is more severe in the 3.0-m sample–detector distance. The data were desmeared by the indirect Fourier transformation algorithm of Moore (1980). This procedure yielded an independent estimate of the forward scatter and radius of gyration. The values obtained from this procedure should be more reliable because the procedure not only considers all the data rather than just those from the Guinier region but also takes into account smearing effects. The values of R_g obtained by the two methods differed by a few percent.

Calculation of Radial Density by Fourier Transformation. Indirect Fourier transformation results in a determination of the length distribution function, $P(r)$ (Moore, 1980). The point at which $P(r)$ becomes zero is an estimate of the maximum dimension of the particle.

At low resolution, icosahedral viruses can be considered as objects with spherical symmetry (Chauvin et al., 1978). In this case, the amplitude, $A(k)$, is equal to $\pm[I(k)]^{1/2}$. The intensity curve for a spherically symmetric object becomes zero at different values of k, and $A(k)$ alternates in sign between the zeros of $I(k)$. The scattering length density of the virus is then given by

$$\rho(r) = 1/r \int_0^\infty kA(k) \sin(kr)\, dk \quad (2)$$

where r is the distance from the center and $\rho(r)$ is the excess scattering length density of virus over solvent (Jacrot, 1981). The desmeared $I(k)$ was used to calculated $\rho(r)$ from the scattering data. The data were truncated around $k = 0.18$ Å^{-1} for the transformation.

Table I: Amino Acid Analysis of KRV Empty Capsids

amino acid	mol %	amino acid	mol %
Asx	12.36	Ile	3.62
Thr	8.26	Leu	6.62
Ser	5.35	Tyr	3.57
Glx	9.40	Phe	3.86
Pro	6.58	His	4.52
Gly	8.89	Trp	3.86
Ala	6.70	Arg	4.24
Val	6.05	Lys	3.76
Met	1.92		

Model Building. Two approaches were used to test models of the virus. In the first case, a model scattering function was compared to the desmeared data, and the parameters of the model were estimated by the nonlinear least-squares procedure of Marquardt (1963). In the other approach, the model function was smeared and then fit to the measured $I(k)$. The two methods yielded essentially the same parameters. The models considered were hollow spheres consisting of a single shell or two concentric shells of different densities.

Results

Amino Acid Analysis. The amino acid composition for the KRV empty capsids is shown in Table I. The value for tryptophan was calculated from the difference between the measured A_{280} and that calculated from the amino acid analysis. The analysis gives $E_{280nm}^{1\%,1cm} = 22.7$ for the empty capsids. The rather high extinction coefficient agrees well with the published values for another parvovirus, MVM (Tattersall et al., 1976).

Molecular Weight. The scattering length per unit mass, $\sum b_i/M$, and the partial specific volume were calculated from the amino acid composition (Jacrot, 1976). Along with a measurement of the incoherent scatter of water and the forward scatter, $I(0)$, in H_2O of a known concentration of capsids, this was used to determine a molecular weight (Jacrot & Zaccai, 1981) of 4.0×10^6 for the KRV empty capsids. The error in the molecular weight comes primarily from the error in the measurement of the absolute concentration and is less than 10%.

Radius of Gyration. The R_g was determined to be 105.1 ± 0.5 Å in D_2O and 103.7 ± 0.5 Å in H_2O. In both cases, the maximum dimension determined from the length distribution function was about 240 Å.

Radial Density Function. The radial density calculated from the amplitude, $A(k)$, in H_2O and D_2O is shown in Figure 2. The Fourier transformation method has the drawback that truncation of the data at $k = 0.18$ Å^{-1} has the effect of introducing spurious oscillations in $\rho(r)$, especially for values of r less than $2\pi/k$, i.e., for $r < 40$ Å.

In both H_2O and D_2O, there is a principal peak in $\rho(r)$ at about 105 Å; however, there is a shoulder indicating a nonzero $\rho(r)$ between 60 and 90 Å, with the main peak occurring between 90 and 120 Å. The relative height of the shoulder compared to the main peak height is larger in H_2O than in D_2O.

The density profiles indicate that while the empty capsid is primarily a shell that extends between $r = 90$ and 120 Å, there may also be an inner shell of smaller density from 60 to 90 Å. To test whether this inner shell is justified by the data or whether it is an artifact introduced by Fourier transformation, the model building approach was used.

Model Building. The results of fitting data to one- and two-shell spheres are shown in Table II and Figure 3. At low values of k, corresponding to very low resolution, both one- and two-shell models agree with the data reasonably well.

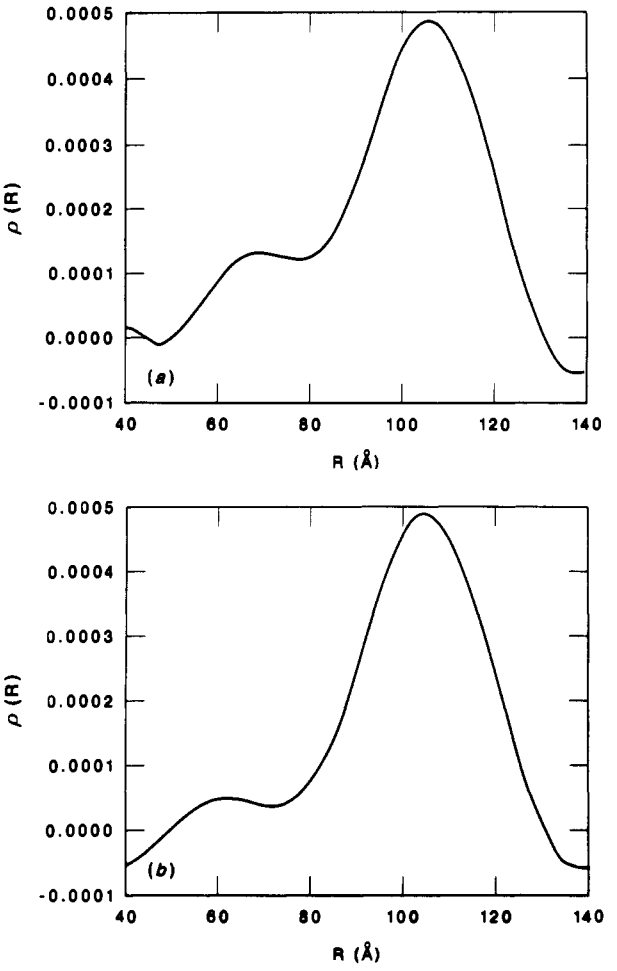

FIGURE 2: Radial density distribution [$\rho(r)$] of protein in KRV empty capsids in H_2O (a) and D_2O (b) calculated as described under Materials and Methods from desmeared values of $I(k)$.

Table II: Structural Parameters for One- and Two-Shell Models of KRV[a]

	one shell	two shells
D_2O	$r_1 = 80.5$ Å	$r_1 = 58.7$ Å
	$r_2 = 123.2$ Å	$r_2 = 90.9$ Å
	$\chi^2 = 101.0$[c]	$r_3 = 121.1$ Å
		$\rho = 0.206$[b]
		$\chi^2 = 4.9$[c]
H_2O	$r_1 = 74.0$ Å	$r_1 = 49.2$ Å
	$r_2 = 124.3$ Å	$r_2 = 91.0$ Å
	$\chi^2 = 46.7$[c]	$r_3 = 120.6$ Å
		$\rho = 0.241$[b]
		$\chi^2 = 4.3$[c]

[a] See Figure 4 for definitions of r_1, r_2, and r_3. [b] Scattering density of inner shell relative to outer shell (=1). [c] Reduced χ^2 assuming 40° of freedom.

However, at higher resolution, a considerably better fit is made by the two-shell model. The values of reduced χ^2 obtained for each model can be used to determine whether the addition of a second shell is significant. An F test, with approximately 40° of freedom, shows that the second shell is extremely significant. Also striking is the fact that the parameters obtained from model building agree with the density profiles obtained from Fourier transformation.

The results show that the KRV empty capsid consists of a primary shell that extends from 90 to 121 Å and a second shell extending inward from 90 to about 58 Å as seen in D_2O and to 50 Å as seen in H_2O. The difference between the inner radius in H_2O and D_2O is primarily due to the fact that the scattered intensity is relatively insensitive to moderate changes

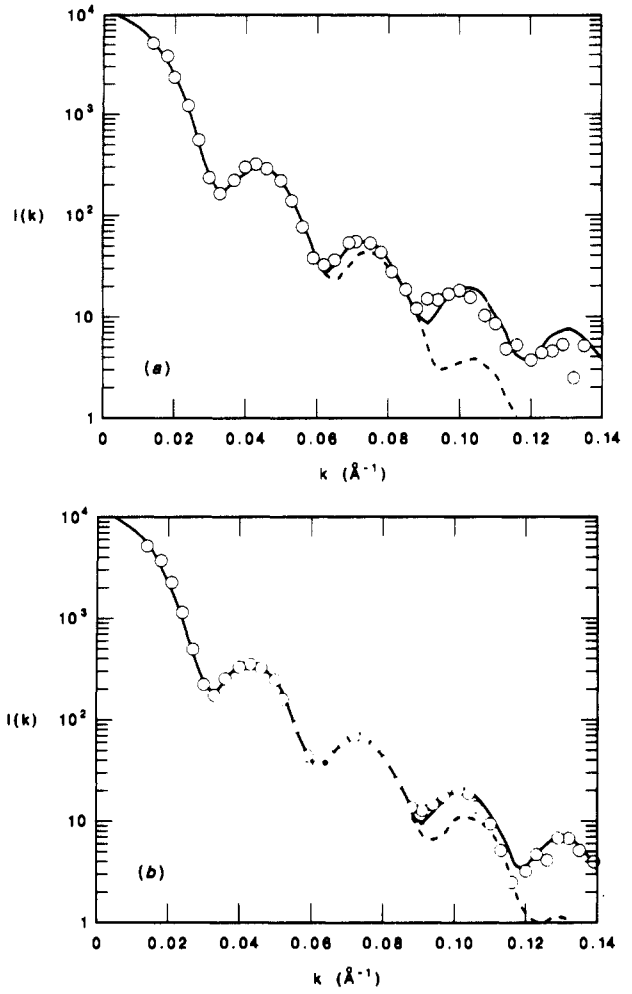

FIGURE 3: Desmeared scattering curves for KRV empty capsids (16.8 mg/mL) in H_2O (a) and D_2O (b) compared to model scattering curves for single-shelled (---) or double-shelled (—) capsids with the properties described in Table II.

in this parameter. Relative to the outer shell, the inner shell has a scattering density of 0.19 in D_2O and 0.24 in H_2O. These results are summarized in the model of the KRV capsid structure in Figure 4.

Discussion

The molecular weight of the empty capsids is calculated to be 4.0×10^6 from the forward scatter. Given that the empty capsid consists primarily of B protein [M_r(B) = 64K] and a small amount of protein A [M_r(A) = 80K] (Mitra et al., 1982), we calculate that it has 60 subunits, suggesting a triangulation number of 1. Assuming 60 subunits, the number of copies of protein A can be estimated to be 10 from the molecular weight by

$$n_A M_r(A) + (60 - n_A) M_r(B) = 4.0 \times 10^6 \quad (3)$$

and in agreement with earlier estimates of the A protein content of parvovirus capsids (Tattersall et al., 1976).

The appearance of 32 capsomeres by electron microscopy led to the conclusion that the virus has a symmetry of $T = 3$ (Vasquez & Brailovsky, 1965; Karasaki, 1966), for which a minimum of 180 protein copies per virus capsid would be required (Caspar & Klug, 1962), inconsistent with the observed molecular weight. However, if each protein has two domains on the surface, one of which was close to the vertex (5-fold axis) and the other close to the center of the icosahedral face (3-fold axis), then it would be possible to observe 32 capsomeres, since one would see 20 face clusters and 12 vertex

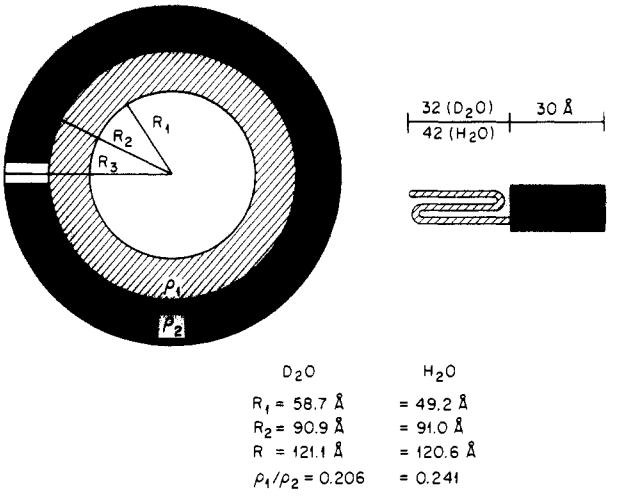

FIGURE 4: Cross section of a model structure for empty capsids of KRV. The hatched ring bounded by R_1 and R_2 is a less dense inner shell, and the solid ring bounded by R_2 and R_3 is the denser outer shell. ρ_1 and ρ_2 refer to scattering densities of the inner and outer shells, respectively. At right is a schematic illustration of a single capsomere emphasizing the highly folded nature of the polypeptide chains of the inner shell.

clusters of domains. Multidomained coat proteins have been observed in tomato brushy stunt virus (Olson et al., 1983; Harrison et al., 1978).

From the neutron scattering data obtained in H_2O and D_2O, we can make predictions about the composition of two shells of protein in the capsid. Generally, the R_g for a soluble protein or complex of proteins is smaller in D_2O than in H_2O due to the presence of hydrophilic groups on the exterior. These groups have a higher scattering length density and lower contrast in D_2O than do other amino acids (Jacrot, 1976). In the case of KRV empty capsids, the radius of gyration is slightly smaller in H_2O, suggesting the presence of hydrophilic amino acids on the inside.

The scattering mass of the virus that contributes to the overall scattering is defined by

$$\sum b_i - \rho_s V \quad (4)$$

where b_i is the sum of the scattering lengths of the amino acids, ρ_s is the scattering length density of the solvent, and V is the excluded volume. The fraction of this scattering mass in the interior shell (f_{inner}) can be calculated from the parameters of the model as follows:

$$f_{inner} = \frac{\rho_1 V_{inner}}{\rho_1 V_{inner} + \rho_2 V_{outer}} = \frac{(\rho_1/\rho_2)(r_2^3 - r_1^3)}{(\rho_1/\rho_2)(r_2^3 - r_1^3) + (r_3^3 - r_2^3)} \quad (5)$$

where ρ_1 and ρ_2 are the scattering densities of the inner and outer shells, respectively, and r_1, r_2, and r_3 are radii depicted in Figure 4. The value of f_{inner} was calculated from the data to be 0.13 in H_2O and 0.09 in D_2O. The lower value in D_2O is consistent with the fact that basic amino acids have a higher contrast in H_2O than in D_2O relative to the bulk of amino acids and suggests that the inner shell, which may interact with DNA, consists of peptide chains containing large numbers of basic amino acids.

The contribution of the basic amino acids, Lys, Arg, and His, to the total scattering mass (f_{basic}) can also be calculated from the amino acid analysis data by the following formula:

$$f_{basic} = \frac{(\sum b - \rho V)_{basic\ residues}}{(\sum b - \rho V)_{total\ residues}} \quad (6)$$

Assuming that the protons of basic residues fully exchange

and, for the virus as a whole, 80% of the labile protons exchange, this ratio turns out to be 0.12 in H_2O and 0.10 in D_2O, in good agreement with the observed values for f_{inner}. This also suggests that most of the basic amino acids are in the interior shell.

On the basis of the data obtained and a knowledge of the protein composition of empty capsids of KRV, it is possible to speculate somewhat on the contributions of the capsid proteins to the inner shell. From an average of the scattering density of the inner shell in H_2O and D_2O, we estimate that 11% of the scattering mass of the capsid is in this shell. While it is possible, as proposed earlier (Tattersall et al., 1977), that the basic regions of protein A may serve a DNA binding function and thus be oriented on the inside of the capsid, it is clear that this cannot solely constitute the inner shell because it only accounts for 4% of the capsid mass. Thus, we feel that a significant contribution to the inner shell of protein is made by B (and/or C).

Eleven percent of the capsid mass would correspond to 440 kDa of protein or, assuming 60 protein molecules per capsid, side chains of about 70 amino acids per protein if each protein contributes equally to the inner shell. Since the inner shell is only 40 Å thick, a distance equivalent to 27 residues of helix or 11 residues of fully extended chain, it is probable that this chain loops back upon itself as depicted in Figure 4.

If the region of A that is nonhomologous with B is entirely in the inner shell together with a common region of A and B (and/or C in full capsids), 2000 of the 4400 inner shell amino acids would be contributed by A in 200 amino acid chains with the remainder supplied by chains approximately 40 residues long from regions common to A and B. We favor this type of model as it is consistent with a possible DNA binding role for the basic A-specific region (Tattersall et al., 1977).

The distribution of protein A in the capsid of KRV cannot be determined by studies of the type done here. Paradiso (1983) has recently suggested that the A protein molecules in the empty capsid of H-1 are situated in close proximity if not in contact with each other. This would eliminate the problem of symmetrically placing 10 points on an icosahedron and would be consistent with the model presented here. Crystallographic studies would be necessary to investigate this possibility more closely; however, if protein A does serve a DNA binding role and if it is clustered in one region of the capsid, the distribution of DNA in full capsids should be similarly asymmetrically clustered. We intend to examine this possibility by small-angle neutron scattering of full capsids.

The importance of first studying empty capsids of KRV is that the distribution of protein can be examined without the interfering effects of scattering due to nucleic acid present in full virions. It is possible to largely eliminate the contribution of nucleic acids by the use of contrast variation (Jacrot, 1976), but the scattering signal from protein is reduced by at least an order of magnitude at the match point for DNA, making structural studies in this detail impractical. Further, several features of empty capsids distinguish them from full virions and suggest possible differences in organization. First, empty capsids are much less susceptible to proteolytic degradation (Tattersall et al., 1977) and alkaline destabilization (Wobbe et al., 1983) than full capsids while the latter are refractile to chemical cross-linking agents compared to empties (Paradiso, 1983). Second, full capsids appear to undergo a proteolytic modification process (Clinton & Hayashi, 1975, 1976) which has not been reported to occur in empty capsids. On the other hand, empty capsids and mature full virions are similar in their hemagglutinating capacities (Tattersall et al., 1976), implying some structural similarity. The differences implied by susceptibility to proteolysis and cross-linking may, in fact, be limited to structural features of the outer surface and would not necessarily imply a different internal organization. Such differences can be explored by a complementary study on full virions.

Acknowledgments

We are grateful to Claude Stringer of the Biology Division, ORNL, for performing amino acid analyses, to D. P. Allison of the Biology Division for performing electron microscopy of the empty and full capsids, and to Marie Pickard for assistance in preparing the manuscript. We also thank Peter Timmins and G. Zaccai of the Institut Laue-Langevin, Grenoble, France, for useful discussions. Some of the model smearing calculations were done by using the computational facilities of the Biology Department, Brookhaven National Laboratory.

References

Caspar, L. D., & Klug, A. (1962) *Cold Spring Harbor Symp. Quant. Biol. 27*, 1–24.

Chauvin, C., Witz, J., & Jacrot, B. (1978) *J. Mol. Biol. 124*, 641–651.

Clinton, G. M., & Hayashi, M. (1975) *Virology 66*, 261–267.

Clinton, G. M., & Hayashi, M. (1976) *Virology 74*, 57–63.

Doc-Nguyen, H., Rosenblum, E. N., & Ziegel, R. F. (1966) *J. Bacteriol. 92*, 1133–1140.

Harrison, S. C., Olson, A. J., Schutt, C. E., Winkler, F. K., & Bricogne, G. (1978) *Nature (London) 276*, 368–376.

Jacrot, B. (1976) *Rep. Prog. Phys. 39*, 911–953.

Jacrot, B. (1981) *Compr. Virol. 17*, 129–181.

Jacrot, B., & Zaccai, G. (1981) *Biopolymers 20*, 2413–2426.

Jacrot, B., Chauvin, C., & Witz, J. (1976) *Nature (London) 266*, 417–421.

Karasaki, S. (1966) *J. Ultrastruct. Res. 16*, 109–122.

Koehler, W., Hendricks, R. W., Child, H. R., King, S. R., Lin, J. S., & Wignall, G. D. (1981) in *Scattering Techniques Applied to Supramolecular and Non-Equilibrium Systems* (Chen, S. N., Chu, B., & Nossal, R., Eds.) pp 75–80, Plenum Press, New York.

Marquardt, D. W. (1963) *J. Soc. Ind. Appl. Math. 11*, 431–441.

Mitra, S., Snyder, C. E., Bates, R. C., & Banerjee, P. T. (1982) *J. Gen. Virol. 61*, 43–54.

Moore, P. B. (1980) *J. Appl. Crystallogr. 13*, 168–175.

Olson, A. J., Bricogne, G., & Harrison, S. C. (1983) *J. Mol. Biol. 171*, 61–94.

Paradiso, P. R. (1983) *J. Virol. 46*, 94–102.

Peterson, J. L., Dale, R. M. K., Karess, R., Leonard, D., & Ward, D. C. (1978) in *Replication of Mammalian Parvoviruses* (Ward, D. C., & Tattersall, P. T., Eds.) pp 431–445, Cold Spring Harbor Laboratory, Cold Spring Harbor, NY.

Rhode, S. L., & Pardiso, P. R. (1983) *J. Virol. 45*, 173–184.

Tattersall, P., & Ward, D. C. (1978) in *Replication of Mammalian Parvoviruses* (Ward, D. C., & Tattersall, P. T., Eds.) pp 3–12, Cold Spring Harbor Laboratory, Cold Spring Harbor, NY.

Tattersall, P., Caute, P. J., Shatkin, A. J., & Ward, D. C. (1976) *J. Virol. 20*, 273–289.

Tattersall, P. T., Shatkin, A. J., & Ward, D. C. (1977) *J. Mol. Biol. 111*, 375–394.

Vasquez, C., & Brailovsky, C. (1965) *Exp. Mol. Pathol. 4*, 130–140.

Wobbe, C. R., Mitra, S., Allison, D. P., & Ramakrishnan, V. (1983) *Fed. Proc., Fed. Am. Soc. Exp. Biol. 42*, 2139.